A Kinetic Study of the Thermal Degradation of Chitosan-Metal Complexes

Edelio Taboada,[1] Gustavo Cabrera,[2] Romel Jimenez,[3] Galo Cardenas[4]

[1]*Universidad Católica de Temuco, Facultad de Ingeniería, Escuela de Ingeniería Ambiental, Campus Norte, Av. Rudecindo, Ortega 02950, Casilla 15-D, Temuco, Chile*
[2]*Universidad Adolfo Ibáñez, Escuela de Negocios, VentureL@b, Diagonal Las Torres 2700, Santiago de Chile, Chile*
[3]*Departamento de Ingeniería Química, Universidad de Concepción, Facultad de Ingeniería, Concepción, Chile*
[4]*Departamento de Polímeros, Universidad de Concepción, Facultad de Ciencias Químicas, Concepción, Chile*

Received 11 September 2008; accepted 4 May 2009
DOI 10.1002/app.30796
Published online 30 June 2009 in Wiley InterScience (www.interscience.wiley.com).

ABSTRACT: The thermal degradation of metal complexes formed by chitosan with Cu(II), Ni(II), Co(II), and Hg(II), at different metal concentrations, was studied by thermogravimetric analysis in a nitrogen atmosphere over the temperature range 25–800°C. The results indicate that thermal degradation of chitosan and chitosan-metal ion complexes could be of one or two-stage reaction. In the thermal degradation of chitosan with metal complexes, the temperature of initial weight loss and the temperature of maximum weight loss rate decrease. Fourier transform infrared spectroscopy was used to probe the interaction of chitosan with metal ions. The bands of —N—H, —C=O, —C—O—C— groups of chitosan are shifted or change their intensity in the presence of metal. These changes in the characteristic bands are taken as evidence of the influence of metal ions on the thermal stability of chitosan. Broido's method was employed to evaluate the activation energies as a function of the degree of degradation. The presence of metal ions provoked a decrease in the thermal stability of chitosan, which became more marked when the concentration of metal was increased. The dynamic study showed that the apparent activation energy values of the main stage of the thermal degradation of chitosan-metal complexes decrease as the strength of the polymer-metal interaction increases. © 2009 Wiley Periodicals, Inc. J Appl Polym Sci 114: 2043–2052, 2009

Key words: chitosan; metal complex; thermal degradation; activation energy; Broido's method

INTRODUCTION

Chitosan, poly-β(1-4)-2-amino-2-deoxy-D-glucopyranose is a biopolymer obtained by total or partial N-deacetylation of chitin, poly-β(1-4)-2-acetamide-2-deoxy-D-glucopyranose, the main constituent of crustacean shells. Partial deacetylation produces a heteropolymer consisting of glucosamine and *N*-acetylglucosamine sugar residues.

Chitosan is characterized by a strong affinity for transition metals. This property makes it attractive for use in water treatment.[1–3] Furthermore, when chitosan is employed as a metal retention resin, it forms complexes with dangerous heavy metals from solution.[4,5] In addition, chitosan-metal complexes can be used in heterogeneous catalysis for applications in the fields of hydrogenation, oxidation and fine chemical synthesis reactions.[6] All these reactions are favored by the increase of the temperature. For this reason the thermal behavior of the polymer-metal complexes submitted to these conditions must be known to prevent side reactions and/or polymer degradation.

Once the chitosan has fulfilled such purposes, it remains as a residue which must be treated as solid waste. One treatment option is to dispose of the solid waste in a sanitary backfill. This option is not advisable because the high concentration of heavy metals can affect the operation of the backfill and contaminate the groundwater. The thermal degradation of these solid wastes seems to be a better disposal solution because the process produces energy and the metallic residues can be confined or reused.

Thermogravimetric analysis is a very widespread technique. For instance, it has been extensively employed to study chitosan degradation and stability.[3,7–12] Nevertheless, a survey of the literature shows that thermal studies of chitosan-metal complexes are rare.[13] We used this technique to observe the changes that are produced in different chitosan-metal complexes during the pyrolysis process, in a nitrogen atmosphere, with different concentrations of metallic ions. To determine the kinetic parameters of the degradation processes, the method developed by Broido[14] was utilized.

Correspondence to: E. Taboada (etaboada@uctemuco.cl).
Contract grant sponsor: DGIUCT 2006-2-04.

The thermal degradation of the chitosan-metal complexes is a complex phenomenon. The metal ions catalyze the degradation and the process is affected by the kind and concentration of metal ions, the structure of complex, the strength of the polymer-metal interaction, etc.

The aim of this study was to contribute to the knowledge of the pyrolysis of chitosan-metal complexes. A better understanding of this process could help to encourage the industrial application of these complexes and their final processing as waste.

MATERIALS AND METHODS

Materials

Chitosan was obtained in our laboratories with a degree of deacetylation of 96.5% and a molecular weight of 131,000 g/mol. The methodology used is an adaptation of that presented in a previous work.[4] The modifications consist in the reduction of the period of deacetylation to 90 min with the addition of 10% $NaBH_4$ to reduce oxidation. Chitosan was used in the form of a powder.

All chemicals used were pure grade: NaOH and HgCl from Merck (Merck S.A., Santiago de Chile, Chile); $CuNO_3{\cdot}3H_2O$, $NiNO_3{\cdot}6H_2O$ and $CoNO_3{\cdot}H_2O$ from Scharlau Chemie (Equilab Ltda., Santiago de Chile, Chile).

Analysis of the degree of acetylation (DA)

The degree of acetylation was determined by the use of RMN ^1H in the liquid state according to the method described by Brugnerotto et al.[15,16]

The RMN ^1H spectra were performed in the AC 300 Bruker Spectrometer (Bruker Corporation, Germany) with a controller processor, coupled to an ASPECT 3000 computer and a variable temperature system. Sodium 4.4-dimethyl-4-sylapentane sulphonate (SDS) was used as external reference.

Determination of the molecular weight

The molecular weight of the chitosan was determined by the viscometric technique. Using the Mark-Houwink equation and [η] values obtained in static experiment it was possible to determine the average viscometric molecular weight (M_V).

$$[\eta] = K(\bar{M}_v)^a$$

The Mark-Houwink parameters $K = 0.076$ (g/mL) and $a = 0.76$ used were determined by Brugnerotto et al.[15] for the chitosan dissolved in the solvent system CH_3COOH 0.3 M/CH_3COONa 0.2 M at 25°C. The intrinsic viscosity [η] of chitosan samples was measured with an Ostwald viscometer at 25°C ± 0.05°C using chitosan concentrations ranging from 0.5×10^{-3} g/mL to 2×10^{-3} g/mL.

Preparation of chitosan-metal complexes

The chitosan-metal complexes were prepared from solutions of copper (pH = 5.0), nickel (pH = 5.5–6.5), cobalt (pH = 4.0–5.0) and mercury (pH = 3.0–4.0) ions with concentrations of 50, 600, and 2000 mg/L, without adjustment of the pH. The complexes were synthesized by mixing 25 mL of solutions containing ions with 25 mg of polymer in solid state. Contact was maintained for 24 h at 25°C in an orbital shaker with temperature control. The solid polymer-metal complexes were filtered and the metal concentrations in the filtered solutions were determined. The solid was dried in a vacuum oven at 60°C for 24 h.

Determination of metal concentration

Elemental analyses were performed in the Chemical Analysis Laboratory of the Chemical Science Faculty at the University of Concepción. The metal concentrations were determined from solutions in a Unican M Series Atomic Absorption equipment (Thermo Fisher Scientific) with hollow cathode lamp.

Thermogravimetric analysis

Thermogravimetric experiments were carried out in a Cahn VersaTherm equipment (Thermo Fisher Scientific) with a temperature control microprocessor and a data station for thermal analysis. The mass of the samples fluctuated between 3 and 5 mg. The pyrolysis was carried out over a temperature range from 25 to 820°C with a heating rate of 10°C/min under nitrogen flow. The mass of the sample was registered continuously as a function of temperature.

Fourier transform infrared (FTIR) analysis

Fourier transform infrared (FTIR) spectra were measured using FTIR Nicolet Magna 5PC spectrophotometer (Thermo Fisher Scientific) coupled to a PC with software ("OMNIC") to data analysis. The KBr disks were prepared by thorough blending of the KBr with dried polymer at 2% concentration. Spectra were recorded at a resolution of 2 cm^{-1} and with an accumulation of 128 scans.

THEORETICAL APPROACH

The kinetic parameters of the thermal decomposition reaction can be evaluated by dynamic and isothermal experiments. In the former case, the sample is heated from room temperature to complete decomposition at a linearly programmed rate, while in the

latter case several isothermal experiments are carried out for different periods of time at a temperature close to the degradation temperature.

Various methods exist for studying the thermal decomposition of polymers. In this work Broido's method was utilized.[14]

The development of this method begins by supposing that a pure solid substance, when it is heated in a vacuum, suffers pyrolysis by means of a reaction in which some of the products are volatile.

The progress of the reaction can be determined by continuously weighing the samples. The weight W_t at any time t, is related to the fraction of the initial number of molecules which have not yet decomposed, y, by means of the equation:

$$y = \frac{N}{N_0} = \frac{(W_t - W_\infty)}{(W_0 - W_\infty)} \tag{1}$$

If the pyrolysis is carried out isothermically, the velocity of the reaction is given by:

$$\frac{dy}{dt} = ky^n \tag{2}$$

where n is the reaction order. The velocity constant k changes with absolute temperature according to the equation of Arrhenius.

$$k = A \cdot e^{-E/RT} \tag{3}$$

If the temperature is a linear function of t, then

$$T = T_0 + u \cdot t \tag{4}$$

u is the heating rate. The first derivative of this equation is:

$$dT = u \cdot dt \tag{5}$$

This rearranges to:

$$\frac{dy}{y^n} = -\left(\frac{A}{u}\right) \cdot e^{-\frac{E}{RT}} dT \tag{6}$$

The thermogravimetric analysis curve for this reaction represents the last equation integrated from a temperature T_0, where $y = 1$, to a temperature for another value of y.

$$\int_y^1 \frac{dy}{y^n} = -\frac{A}{u} \int_T^{T_0} e^{-\frac{E}{RT}}\, dT = \frac{A}{u} \int_{T_0}^{T} e^{-\frac{E}{RT}} dT \tag{7}$$

The main consideration of this method is that the reaction is of the first order. With this supposition the left side of the reaction can be resolved.

$$\int_y^1 \frac{dy}{y^n} = \int_y^1 \frac{dy}{y} = -\ln y = \ln\left(\frac{1}{y}\right) \tag{8}$$

There are various methods for resolving the right side of the equation. Broido's method is based on approximations done by other authors. We have utilized the approximations introduced by Horowitz and Metsger.[16]

$$e^{-\frac{E}{RT}} \approx \left(\frac{T_m}{T}\right)^2 e^{-\frac{E}{RT_m}} \tag{9}$$

T_m is the temperature at which the maximum reaction velocity occurs. Introducing this approximation has

$$Ln\frac{1}{y} = \frac{A}{u} \int \left(\frac{T_m}{T}\right)^2 e^{-\frac{E}{RT}} dT \tag{10}$$

Changing variable has

$$x = \frac{1}{T} \quad \Rightarrow \quad dx = \frac{1}{T^2} dT \quad \Rightarrow \quad dT = -\left(\frac{1}{x^2}\right) dx$$

$$\ln\frac{1}{y} = \frac{A}{u} T_m^2 \int x^2 e^{-\frac{E}{R}X} \left(-\frac{1}{x^2}\right) dx \tag{11}$$

$$\ln\frac{1}{y} = \frac{A \cdot R \cdot T_m^2}{E \cdot u} \cdot e^{-\frac{E}{R}X}$$

$$\ln\frac{1}{y} = \frac{A \cdot R \cdot T_m^2}{E \cdot u} \cdot e^{-\frac{E}{R}\left(\frac{1}{T}\right)}$$

$$\ln \ln\frac{1}{y} = -\frac{E}{R}\left(\frac{1}{T}\right) + \ln\left(\frac{A \cdot R \cdot T_m^2}{E \cdot u}\right) \tag{12}$$

This equation can be represented by:

$$\ln \ln\frac{1}{y} = -\frac{E}{R}\left(\frac{1}{T}\right) + \text{const.}$$

Equation 12 is a straight line. The gradient of the graph $\ln \ln \frac{1}{y}$ vs. $\left(\frac{1}{T}\right)$ is the activation energy E_a and the intercept is frequency factor A.

RESULTS AND DISCUSSION

FTIR analysis of chitosan-metal complexes

Spectroscopy in the infrared region was used to monitor structural changes and the principal interactions between chitosan and the metal ions before thermal degradation. The spectra of chitosan and chitosan with Cu(II), Hg(II), Co(II) and Ni(II) are shown in Figure 1. The characteristic FTIR bands of the samples are listed in Table I.

FTIR analysis of chitosan

In the region of 3000–3700 cm^{-1} of the spectrum, chitosan exhibits a strong, broad band due to the

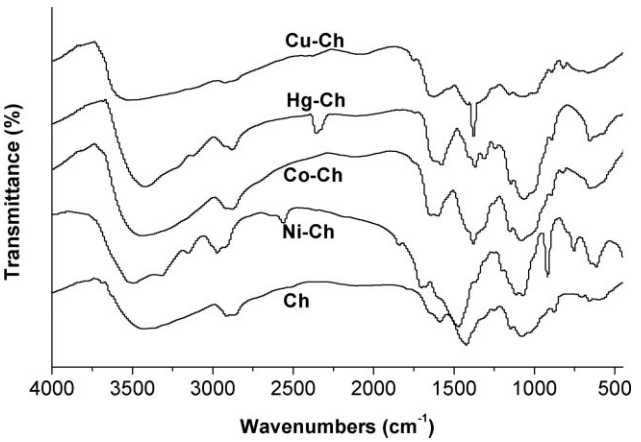

Figure 1 FTIR spectra of chitosan and chitosan metal complexes.

axial stretching of OH and N—H bonds centred at 3425 cm^{-1}. This band is broad because of the hydrogen bonds. The OH band overlaps the N—H stretching band. The bands observed at 2915 and 2865 cm^{-1} correspond to the axial stretching of C—H bonds.

The amide I band (C=O) characteristic of chitosan with acetylated units appears at 1653 cm^{-1}. The band at 1590 cm^{-1} is produced by the overlapping of in-plane bending (scissoring) of N—H of amine chitosan groups and the amide II band.

The bands at 1420 cm^{-1} result from C—N axial stretching and the bands corresponding to the polysaccharide skeleton, including the vibrations of the glycosidic bonds (C—O and C—O—C stretching) were observed in the range 1153–897 cm^{-1}.

FTIR analysis of chitosan-Cu(II) complexes

The main bands observed in the chitosan spectrum are also present in the chitosan Cu(II) spectrum. The principal changes produced by the interaction between chitosan and Cu(II) is the overlapping of the amide I band and the band due to angular deformation of —N—H bonds observed at 1630 cm^{-1}. This overlapping is due to the interaction of Cu(II) with amine and C=O groups. These changes are the principal evidence of the influence of the Cu(II) on the thermal stability of chitosan. The strong band at 1380 cm^{-1} correspond to the symmetrical stretching of the N=O group from the salt $CuNO_3$.

FTIR analysis of chitosan-Ni(II) complexes

When chitosan interacts with Ni(II) ions the band becomes unfolded in the region of 3000 to 3700 cm^{-1}, and the stretching of O—H is observed at 3440 cm^{-1}. Chitosan has N—H amide bonds and N—H amine bonds. The asymmetrical and symmetrical N—H stretching vibrations band becomes unfolded in the presence of Ni(II) at 3270 and 3108 cm^{-1}.

When chitosan is charged with Ni(II) ions the amide I band appears at a high wave number (1660 cm^{-1}). Electron-attracting groups attached to the nitrogen increase the frequency of absorption since they effectively compete with the carbonyl oxygen for the electrons of the nitrogen, thus increasing the force constant of the C=O bond. Another band is unfolded at 1633 cm^{-1} corresponding to the N—H bonds.

FTIR analysis of chitosan-Co(II) complexes

The main bands observed in the chitosan spectrum are also present in the chitosan Co(II) spectrum. However, due to the interaction of Co(II) with the nitrogen, when chitosan is charged with Co(II) ions the amide I band (C=O) and the band corresponding to the N—H bonds appears at high wave numbers (1660 and 1605 $cm^{-1,}$ respectively). Changes are also observed in the intensities of the bands

TABLE I
Characteristic FTIR Bands of Chitosan and Chitosan-Metal Complexes

Sample	FTIR (Wave number, cm^{-1})
Chitosan	3440 cm^{-1} (—OH, —NH); 2915 cm^{-1} and 2865 cm^{-1} (—C—H); 1653 cm^{-1} (—C=O, amide I); 1590 cm^{-1} (—N—H); 1420 cm^{-1} (—C—N—) coupled with 1380 cm^{-1} (—N—H); 1155-875 cm^{-1} (skeleton: C—O and —C—O—C—)
Ch-Cu	3540 cm^{-1} (—OH), shoulder 3132 (—NH); 2915 cm^{-1} and 2875 cm^{-1} (—C—H); 1630 cm^{-1} (—C=O and —N—H overlaps); 1420 cm^{-1} (—C—N—) coupled with 1380 cm^{-1} (—N—H); 1155-875 cm^{-1} (skeleton: C—O and —C—O—C—)
Ch-Co	3440 cm^{-1} (—OH, —NH); 2915 cm^{-1} and 2875 cm^{-1} (—C—H); 1660 cm^{-1} (—C=O, amide I); 1605 cm^{-1} (—N—H); 1420 cm^{-1} (—C—N—) coupled with 1380 cm^{-1} (—N—H); 1155-875 cm^{-1} (skeleton: C—O and —C—O—C—)
Ch-Ni	3440 cm^{-1} (—OH); 3270 cm^{-1} and 3108 cm^{-1} (—NH); 2915 cm^{-1} and 2875 cm^{-1} (—C—H); 1660 cm^{-1} (—C=O, amide I); 1630 cm^{-1} (—N—H, amide II); 1420 cm^{-1} (—C—N—) coupled with 1380 cm^{-1} (—N—H); 1155-875 cm^{-1} (skeleton: C—O and —C—O—C—)
Ch-Hg	3430 cm^{-1} (—OH); 3250 cm^{-1} and 3132 cm^{-1}(—NH); 2915 cm^{-1} and 2875 cm^{-1} (—C—H); 1630 cm^{-1} (—C=O, amide I); 1590 cm^{-1} (—N—H); 1420 cm^{-1} (—C—N—) coupled with 1380 cm^{-1} (—N—H); 1155-875 cm^{-1} (skeleton: C—O and —C—O—C—)

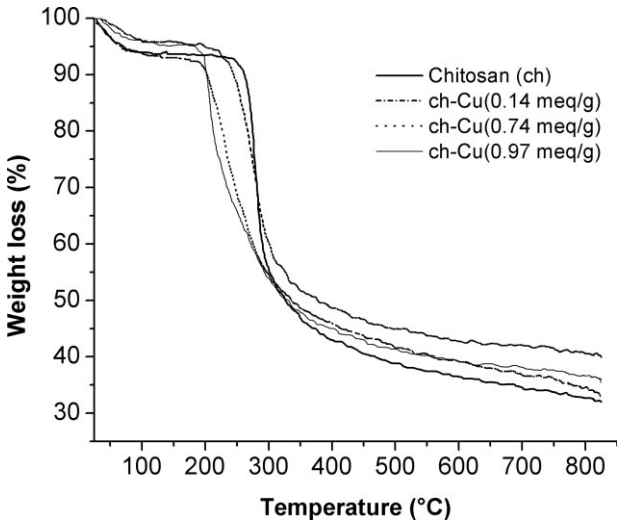

Figure 2 Thermogravimetric analysis de chitosan Cu(II) complexes.

corresponding to C—N axial stretching, N—H angular deformation and the bands corresponding to the polysaccharide skeleton. These changes are taken as evidence of the influence of the cobalt on the thermal stability of chitosan. The band at 1380 cm^{-1} correspond to the symmetrical stretching of the N=O group from the salt $CoNO_3$.

FTIR analysis of chitosan-Hg(II) complexes

When chitosan interacts with Hg(II) ions the bands, in the region of 3000–3700 cm^{-1}, become unfolded and the stretching of O—H is observed at 3430 cm^{-1}. The asymmetrical and symmetrical N—H stretching vibrations band becomes unfolded at 3250 and 3132 cm^{-1}. Another significant change is produce by the interaction of Hg with C=O groups. The amide I band corresponding to the C=O bond is not observed and another band appears at 1630 cm^{-1} due to angular deformation of —N—H.

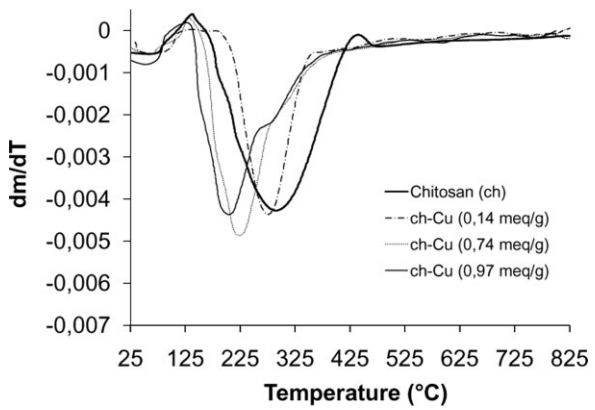

Figure 3 DTG curves of the chitosan Cu(II) complexes.

Thermogravimetric analysis of chitosan—Cu(II) complexes

The TG and the corresponding DTG curves of chitosan Cu(II) complexes are shown in Figures 2 and 3 respectively. The temperatures for the occurrence of the main thermal events and corresponding mass losses are given in Table II. In Figures 2 and 3 it is observed that the first thermal event occurs in the temperature range 25–140°C, where all samples present a mass loss of between 4 and 7%. This is attributed to the evaporation of water, the content of which is a function of the morphology, crystallinity and hydrophilicity of the polymers.[11,17,18] According to the results presented in Figures 2 and 3, the mass losses corresponding to the evaporation of water appear to depend on the presence and number of ions in the polymer chains.

The second thermal event occurs in the temperature range 190–410°C for chitosan. In the presence of Cu(II) ions a displacement toward lower degradation temperatures is observed when the metallic ion

TABLE II
Characteristic Temperatures and Weight Loss (%) for the Thermal Degradation of Chitosan and Chitosan-Metal Complexes

	Temperature (°C)		
	[a]Peak max	Range	Weight loss (%)
First stage			
Chitosan	–	25–140	6.6
chit-Cu (0.14 meq/g)	–	25–140	5.0
chit-Cu (0.74 meq/g)	–	25–140	7.0
chit-Cu (0.97 meq/g)	–	25–140	6.2
chit-Ni (0.05 meq/g)	–	25–140	7.2
chit-Ni (0.34 meq/g)	–	25–140	6.3
chit-Ni (0.67 meq/g)	–	25–140	6.3
chit-Co (0.02 meq/g)	–	25–140	4.0
chit-Co (0.16 meq/g)	–	25–140	4.0
chit-Co (0.36 meq/g)	–	25–140	6.3
a-chit-Hg (<0.05 meq/g)	–	25–140	3.0
b-chit-Hg (<0.05 meq/g)	–	25–140	5.2
chit-Hg (1.17 meq/g)	–	25–140	5.2
Second stage			
Chitosan	295	190–410	51
chit-Cu (0.14 meq/g)	277	180–360	45
chit-Cu (0.74 meq/g)	225	150–400	47
chit-Cu (0.97 meq/g)	208	130–400	50
chit-Ni (0.05 meq/g)	285	200–360	47
chit-Ni (0.34 meq/g)	260	180–380	46
chit-Ni (0.67 meq/g)	257	180–380	45
chit-Co (0.02 meq/g)	284	200–360	48
chit-Co (0.16 meq/g)	269	180–400	48
chit-Co (0.36 meq/g)	260	180–400	46
a-chit-Hg (<0.05 meq/g)	275	180–360	47
b-chit-Hg (<0.05 meq/g)	240	140–320	49
chit-Hg (1.17 meq/g)	235	140–355	54

[a] This temperature was obtained from the differential thermogravimetric analysis.

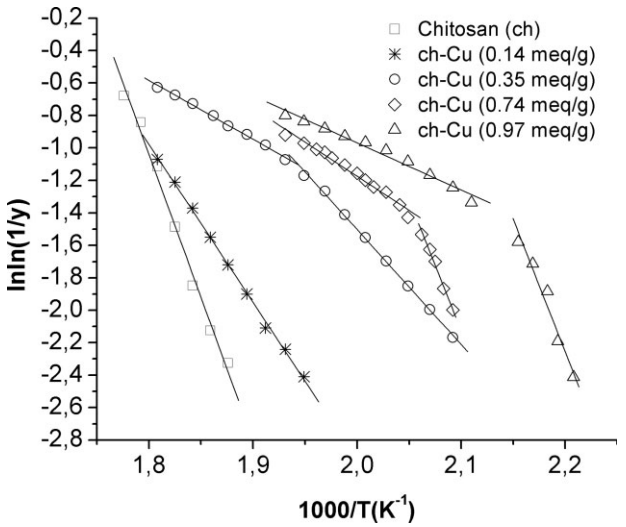

Figure 4 Plots of lnln(1/y) vs $1000*T^{-1}(K^{-1})$ using Broido's equation for chitosan Cu(II) complexes.

concentration is increased. This event is attributed to the thermal degradation of the polymers, including the deacetylation of chitosan. The complete thermal decomposition of the polymers, involving the depolymerization and pyrolitic processes, is attained at temperatures higher than 360 and 400°C for chitosan-metal complexes and 410°C for chitosan. In the decomposition stage corresponding to the range 190–410°C, the mass loss of chitosan is 51% while that of chitosan-metal complexes for the interval 130–380°C ranges from 45 to 50% (Table II).

As may be observed in the TG and DTG curves (Figs. 2 and 3), this stage of thermal decomposition begins at lower temperatures for the chitosan-metal complex samples, showing that these complexes are less thermally stable than chitosan. Indeed, the data in Table II show that the temperature, at which the maximum mass loss occurs, in the second stage of degradation, is dependent on the metal content, with high metallic ion concentration samples presenting lower temperatures.

This effect could be analyzed through the kinetic parameters obtained from Broido's method (Figure 4). For this purpose, only the main degradation process will be presented in each case.

The straight line gradient obtained is directly related to the apparent activation energy (E_a). It may be observed that the gradient, and therefore the E_a, decreases when the metal concentration is increased. This behaviour might be due to the catalytic effect of the Cu (II) ion on the thermal degradation of chitosan. When the metal concentration in the matrix is equal to or higher than 0.35 meq metal/g polymer, the main process occurs in two periods.

The E_a values (see Table III) of the first period are comparable to the E_a values for the degradation process of chitosan without metal. The second period occurs at lower E_a values than the first period. The results indicate that the change in the conformation of chitosan which results from mixing with the metal ion has an effect on the formation of different phases in the polymer, which partly decreases the bond energies of glycosidic linkages in chitosan and consequently leads to its thermal instability.

The E_a values for low metal concentrations (0.14 meq metal/g polymer) are intermediate between those obtained for chitosan without metal, and the second period of the chitosan with high metal concentrations. It may be that this fact is related to the simultaneous occurrence of the two processes, and the E_a value found is an average of the separate processes.

The weight loss values of the complete process are quite similar in all cases. However at 800°C a greater amount of undisturbed solid remained when a polymer-metal complex was assayed. Nevertheless, the

TABLE III
Apparent Activation Energies (E_a) for the Thermal Degradation of Chitosan and Chitosan-Metal Complexes Determined According to Broido's Method

	Period I		Period II	
	Range (°C)	E_a (kJ mol^{-1})	Range (°C)	E_a (kJ mol^{-1})
Chitosan	200–400	146.5 ± 0.7		–
chit-Cu (0.14 meq/g)	240–290	80.8 ± 0.1		–
chit-Cu (0.74 meq/g)	195–215	133.4 ± 1.0	215–235	34.9 ± 0.2
chit-Cu (0.97 meq/g)	175–190	135.9 ± 1.8	190–220	24.1 ± 0.2
chit-Ni (0.05 meq/g)	260–290	114.4 ± 0.4		–
chit-Ni (0.34 meq/g)	230–260	110.6 ± 0.6		–
chit-Ni (0.67 meq/g)	225–255	109.5 ± 0.9		–
chit-Co (0.02 meq/g)	250–290	114.1 ± 0.5		–
chit-Co (0.16 meq/g)	230–275	81.6 ± 0.2		–
chit-Co (0.36 meq/g)	225–270	79.3 ± 0.5		–
a-chit-Hg (<0.05 meq/g)	230–285	86.8 ± 0.1		–
b-chit-Hg (<0.05 meq/g)	215–250	83.4 ± 0.4		–
chit-Hg (1.17 meq/g)	200–215	109.9 ± 1.0	215–245	53.8 ± 0.2

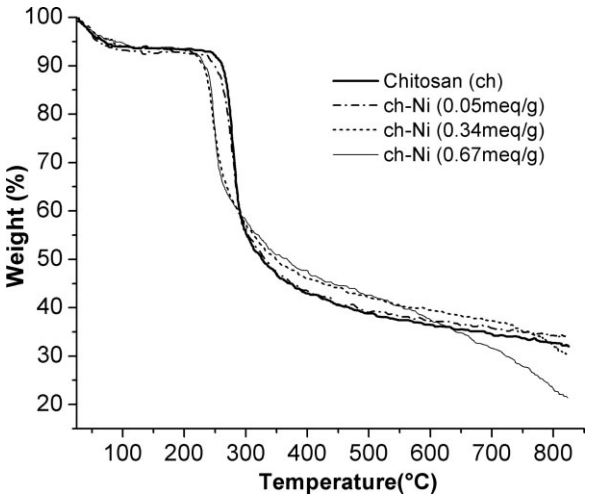

Figure 5 Thermogravimetric analysis de chitosan Ni(II) complexes.

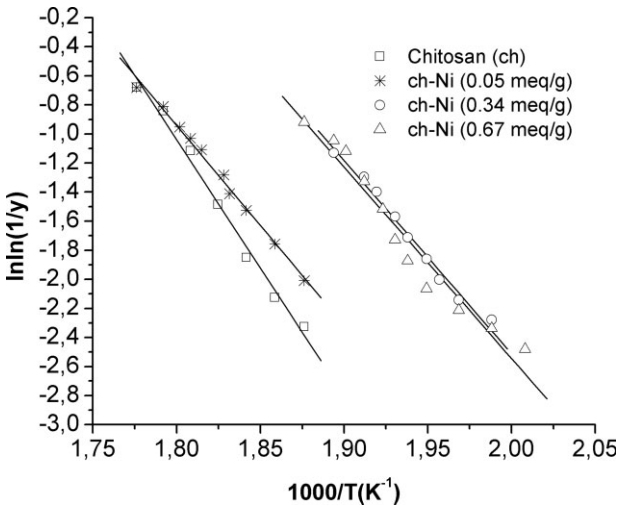

Figure 7 Plots of lnln(1/y) vs $1000*T^{-1}(K^{-1})$ using Broido's equation for chitosan Ni(II) complexes.

residual weight at the end of pyrolysis is not proportional to the initial metal concentration in the complex. For example, a greater weight percentage of residual solid remains at the end of pyrolysis for 0.14 meq metal/g polymer than for 0.97 meq metal/g polymer. This could be connected to the formation of greater amounts of carbon in the former case. This is an interesting aspect for future studies, since it suggests that chitosan may be utilized as alternative source for obtaining carbon fibres.[19] Besides, there are references of metals such as copper and nickel being used as catalysts in these processes.[20]

Thermogravimetric analysis of chitosan—Ni(II) complexes

The TG and the corresponding DTG curves of chitosan Ni(II) complexes are shown in Figures 5 and 6, respectively. The temperatures for the occurrence of the main thermal events and corresponding mass losses are given in Table II. In Figures 5 and 6 it may be observed that the first thermal event occurs in the temperature range 25–140°C, where all samples present a mass loss from 6.3 to 7.2%. This is attributed to the evaporation of water loosely bound to the polymer. The second thermal event occurs at lower temperatures than in chitosan. In the presence of Ni(II) ions a displacement toward lower degradation temperatures is observed when the metallic ion concentration is increased.

The Ni(II) ion also has a catalytic effect on the thermal degradation reaction for chitosan. In Figures 5 and 6, it may be observed that the temperature ranges and the temperature of the maximum rate of degradation shift to lower values when the metal concentration is increased from 0.05 meq metal/mg polymer to 0.34 meq metal/mg polymer.

This effect could be analyzed through the kinetic parameters obtained from Broido's method (Figure 7). For the present purpose, only the main degradation process will be presented.

A decrease of the E_a values during pyrolysis was observed when there were metals present. The E_a

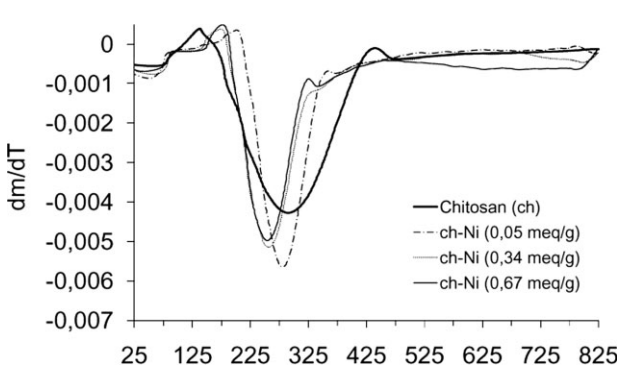

Figure 6 DTG curves of the chitosan Ni(II) complexes.

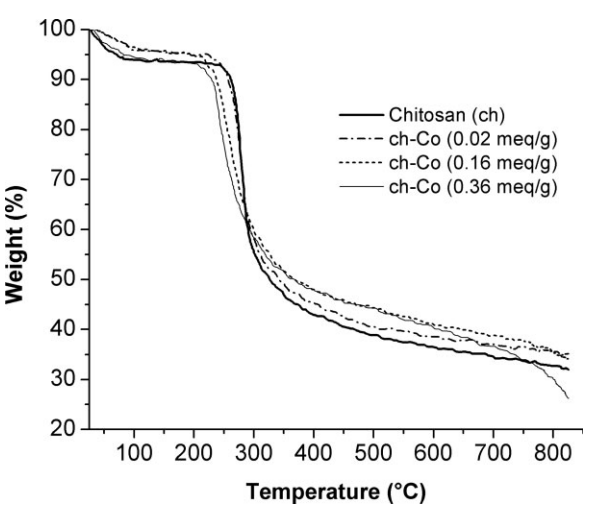

Figure 8 Thermogravimetric analysis de chitosan Co(II) complexes.

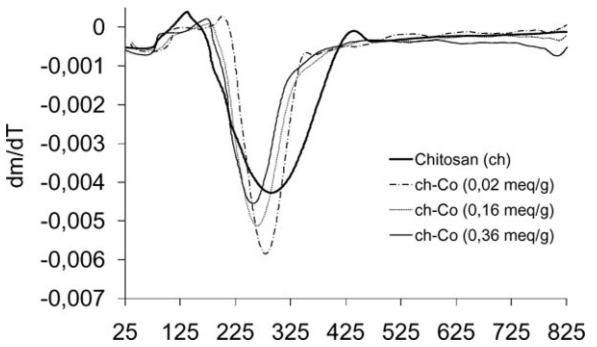

Figure 9 DTG curves of the chitosan Co(II) complexes.

values obtained for Ni (II) were greater than those for Cu (II). Nevertheless, it is interesting to note that the main thermal degradation of chitosan in the presence of Ni (II) occurred in a single phase. This differs from the result obtained for Cu (II) where two phases were observed. The E_a values for Ni (II) and the weight loss associated are practically the same for all concentrations.

It was observed that an increment in the metal concentration above 0.34 meq metal /mg polymer does not produce a major effect on the E_a vales. The weight losses obtained were slightly smaller than for chitosan without metal.

Thermogravimetric analysis of chitosan—Co(II) complexes

The TG and DTG curves of chitosan Co(II) complexes are shown in Figures 8 and 9 respectively. The temperatures for the occurrence of the main thermal events and the corresponding mass losses are given in Table II. In Figures 8 and 9 it may be observed that the first thermal event occurs in the temperature range 25–140°C, where all samples pres-

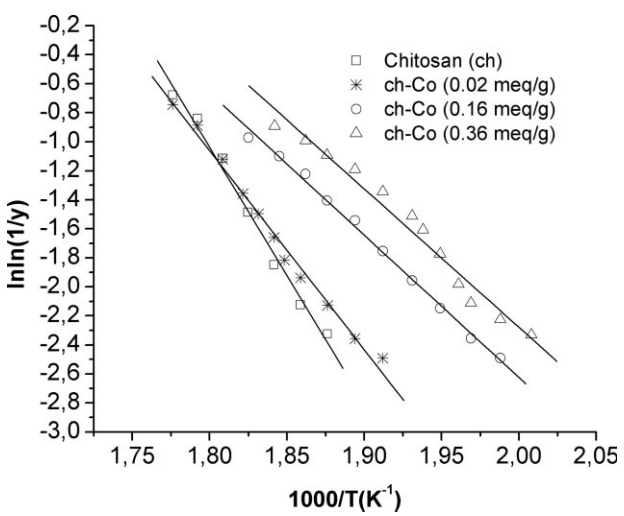

Figure 10 Plots of lnln(1/y) vs $1000*T^{-1}(K^{-1})$ using Broido's equation for chitosan Co(II) complexes.

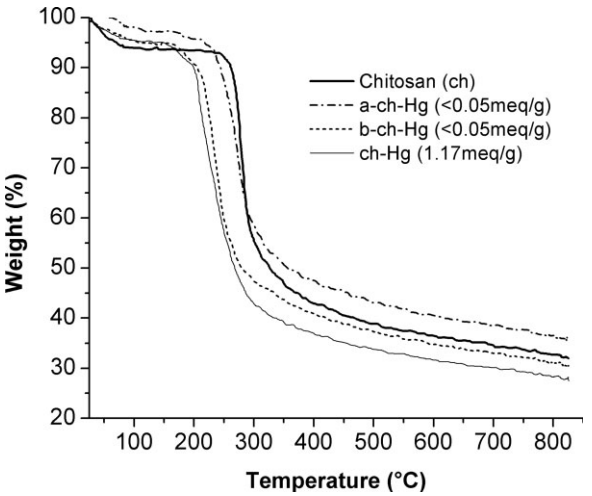

Figure 11 Thermogravimetric analysis de chitosan Hg(II) complexes.

ent a mass loss of between 4.0 and 6.3%. This is attributed to the evaporation of water loosely bound to the polymer. The ranges of temperatures and the temperatures of the maximum rate of the second degradation process are practically equal for the Co (II) and Ni (II), and are reduced when the concentration of metal is increased.

The kinetic parameters obtained from Broido's method (Figure 10) for the main degradation process are presented in Table III. The Co (II) has a better catalytic effect than the Ni (II) because it has smaller E_a values. These activation energy values decrease when the concentration of the metal is increased. They result in an opposite behavior to that obtained for Ni (II). Nevertheless, the E_a values calculated were greater than those obtained for Cu (II).

Thermogravimetric analysis of chitosan Hg (II) complexes

The TG and DTG curves of chitosan Hg(II) complexes are shown in Figures 11 and 12 respectively. The temperatures for the occurrence of the main

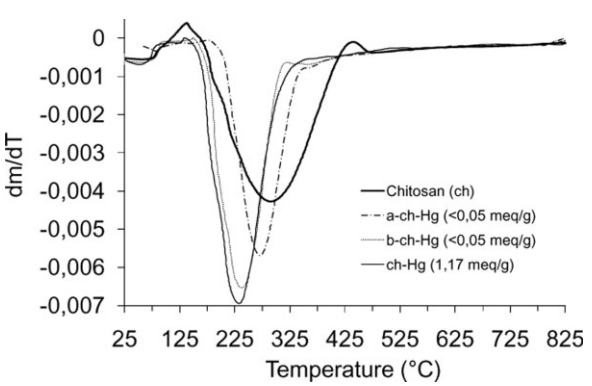

Figure 12 DTG curves of the chitosan Hg (II) complexes.

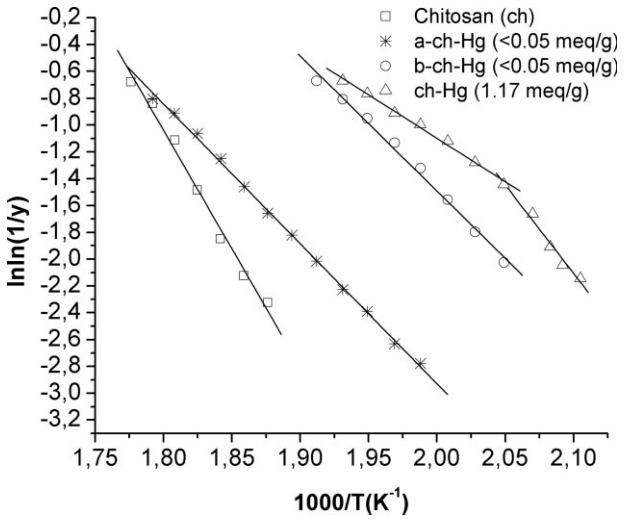

Figure 13 Plots of lnln(1/y) vs $1000*T^{-1}(K^{-1})$ using Broido's equation for chitosan Hg(II) complexes.

thermal events and corresponding mass losses are given in Table II. Chitosan Hg(II) complexes also present a first thermal event in the temperature range 25–140°C, due to the water loosely bound to the polymer. The mass losses for this first stage were from 3.0 to 5.2%. The temperature range and the temperature of the maximum rate for the second degradation process decrease when the concentration of metal is increased, as in the previous cases.

The kinetic parameters obtained from Broido's method (Figure 13) for the main degradation process are presented in Table III. The Hg (II) also showed a catalytic effect on the thermal degradation of chitosan. The E_a values are very similar to Cu (II). Other aspects displaying similarity are: the presence of two degradation periods, only at the higher metal concentration studied; and fact that the percentage of weight losses remains unaltered.

When the apparent E_a values for Ni(II), Co(II), and Cu(II) ions were compared at similar concentrations it was observed that they decrease in the following order: Ni(II) > Co(II) > Cu(II). It's interesting to note that the retention constants obtained in the adsorption experiments showed the inverse order: Ni < Co < Cu.[21] This is in accordance with the principle of Pearson of hard and soft acids and bases[22] which states that hard acids react faster and form stronger bonds with hard bases. The chitosan retention takes place by the hard bases NH_2 and ROH groups, according to the FTIR analysis. Then, the greater the hardness of the metallic ion, the stronger will be the interaction with these ligand groups. The hardness order of the metals studied in this work is the following: Cu (II) > Co (II) > Ni (II). From these results it may be observed a catalytic effect of the metal on the pyrolysis process of the polymer matrix because the stronger is the interaction strength of polymer-metal, the smaller is the apparent activation energy of the degradation process.

The Hg (II) behavior wasn't compared in this case because it doesn't have similar concentration to the others ions in the solid phase. It is known that this metal behaves like a soft acid thus the strength of Hg(II)-chitosan interaction must be weaker. However, in this study it wasn't possible to make a comparison. Finally, it is important to note that an accurate reaction mechanism can't be explained based only on interaction strengths but other aspects such as chitosan-metal complex structure, type of metal and its concentration should be very relevant indeed.

CONCLUSIONS

1. The study of the thermal degradation of chitosan-metal complexes in a nitrogen atmosphere revealed that the presence of Cu, Ni, Co, and Hg ions provoked a decrease in the thermal stability of chitosan.
2. The higher the concentration of metal, the lower the temperature of the maximum degradation rate.
3. Broido's method allowed the apparent activation energies for the thermal degradation of chitosan-metal complexes in dynamic conditions to be determined. However, this method is applied to reactions of the first order. Therefore, in some cases, it was necessary to analyze the whole degradation process in separate and independent phases. This approximation is valid considering a multireaction process.
4. The dynamic study showed a decrease in the apparent activation energy values for the main stage of the thermal degradation of these chitosan-metal complexes when the strength of the polymer-metal interaction is increased. This could be considered as a proof of the catalytic activity of the Cu, Ni, Co, and Hg ions in the thermal degradation of chitosan.

References

1. Guibal, E.; Van Vooren, M.; Dempsey, B. A.; Roussy, J. Sep Sci Technol 2006, 41, 2487.
2. Guibal, E. Sep Purif Technol 2004, 38, 43.
3. Cardenas, G.; Orlando, P.; Edelio, T. Int J Biol Macromol 2001, 28, 167.
4. Taboada, E.; Cabrera, G.; Cardenas, G. J Chilean Chem Soc 2003, 48, 7.
5. Cardenas, G.; Cabrera, G.; Taboada, E.; Miranda, S. P. J Appl Polym Sci 2004, 93, 1876.
6. Guibal, E. Prog Polym Sci 2005, 30, 71.

7. Taboada, E.; Cabrera, G.; Cardenas, G. J Appl Polym Sci 2004, 91, 807.
8. Cardenas, G.; Miranda, S. P. J Chilean Chem Soc 2004, 49, 291.
9. Penichecovas, C.; Arguellesmonal, W.; Sanroman, J. Polym Degrad Stab 1993, 39, 21.
10. Cardenas, G.; Sanzana, J.; Mei, L. H. I. Boletin De La Sociedad Chilena De Quimica 2002, 47, 529.
11. Tang, W. J.; Wang, C. X.; Chen, D. H. Polym Degrad Stab 2005, 87, 389.
12. Pawlak, A.; Mucha, A. Thermochim Acta 2003, 396, 153.
13. Cui, Y. C.; Zhang, L.; Li, Y. Polym Adv Technol 2005, 16, 633.
14. Broido, A. J Polym Sci Part A 1969, 27, 1761.
15. Brugnerotto, J.; Desbrieres, J.; Heux, L.; Mazeau, K.; Rinaudo, M. Macromol Symp 2001, 168, 1.
16. Wendland, W.Thermal Methods of Analysis; Interscience: New York, 1964, Vol. XIX, p 424.
17. de Britto, D.; Campana, S. P. Polym Degrad Stab 2004, 84, 353.
18. Ou, C. Y.; Li, S. D.; Li, C. P.; Zhang, C. H.; Yang, L.; Chen, C. P. J Appl Polym Sci 2008, 109, 957.
19. Bengisu, M.; Yilmaz, E. Carbohydr Polym 2002, 50, 165.
20. Kim, M. S.; Rodriguez, N. M.; Baker, R. T. K. J Catal 1991, 131, 60.
21. Taboada, E. PhD Dissertation, In Facultad de Ciencias Químicas, Universidad de Concepción, Concepción, 2003.
22. Pearson, R. G. J Am Chem Soc 1963, 85, 3533.